ARTICLES

Isolation of Smaller Nanocrystal Au Molecules: Robust Quantum Effects in Optical Spectra

T. G. Schaaff, M. N. Shafigullin, J. T. Khoury, I. Vezmar, R. L. Whetten,* W. G. Cullen, and P. N. First

Schools of Physics and Chemistry, Georgia Institute of Technology, Atlanta, Georgia 30332-0430

C. Gutiérrez-Wing, J. Ascensio, and M. J. Jose-Yacamán†

ININ, Amsterdam 46-202, Col. Hipodromo Condesa, 06100 Mexico DF, Mexico

Received: April 25, 1997; In Final Form: July 15, 1997[⊗]

Five massive gold-cluster molecules have been isolated in high yield and have undergone separate structural characterization, and their electronic structure has been deduced by optical absorption spectroscopy. These new molecules are distinguished by a crystalline (or quasicrystalline) core of densely packed Au atoms, ranging in size from ∼1.1 nm (∼40 atoms) to ∼1.9 nm (∼200 atoms), surrounded by a compact monolayer of various thio (RS) adsorbates. They are obtained as the thermally and environmentally stable products of the reductive decomposition of nonmetallic (−AuS(R)−) polymer in solution, are separated according to size by fractional crystallization or column chromatography, as monitored by high-mass spectrometry, and are characterized structurally by methods including X-ray diffraction (small and large angle), high-resolution electron microscopy, and scanning tunneling microscopy. The optical absorption spectra of dilute solutions of these molecules show size-dependent steplike structure with an onset near the fcc Au interband edge ($\Delta = 1.7$), indicative of transitions to the discrete lowest unoccupied levels of the conduction band. This structure is evident in the smallest clusters even at room temperature, is enhanced at low temperature, and emerges generally as predicted by Kubo's criterion for quantum size effects. It thus *requires no assumption of a transition from the bulk metallic bonding character* to a nonmetallic (rehybridized or oxidized) state.

1. Introduction

Larger metal-atomic clusters A_N are capable of exhibiting a range of ideal properties of great fundamental as well as potential technological significance. Among their *structural properties* are (i) an early onset (a few tens of atoms)[1] of crystalline (or quasicrystalline) structures possessing near-ideal strength and no ductility-malleability property;[2] (ii) stability patterns punctuated at critical sizes corresponding to structural shell-filling "magic numbers",[3] for which the surface structure assumes a simple polyhedral form; and (iii) active surfaces that can be saturated by a definite number of adsorbates without necessarily transforming the cluster's intrinsic structure.[4]

Included among their *electronic properties*, defined (as usual) in relation to the archetypal properties of bulk conductors as "quantum size effects" (QSEs), are (iv) the discrete charge states (Ze) and charging energies of a tiny globular conductor with excess charge delocalized over the surface;[5] (v) the quantized level structure of the conduction band, with levels grouped into an electronic shell structure and classified according to a spherical−spheroidal shell model;[6] and (vi) the diverse transport, optical, and chemical properties derived therefrom.

As a practical matter, the latter QSEs (v) are expected to be important at ordinary temperatures only for sufficiently small clusters, and they can be seriously obscured by the effects of polydispersity. This principle finds simple quantitative expression in the (Kubo) criterion[6] that the (mean) level spacing $\delta(\epsilon_F)$ near the Fermi energy (HOMO−LUMO gaps), as estimated from the bulk density of states, exceeds the characteristic thermal energy

$$\delta(\epsilon_F) \approx \frac{3}{2}\frac{\epsilon_F}{N_A z} > k_B T \qquad (1)$$

where N_A is the number of metal atoms and z their valence. In the case of gold ($z = 1$), $\delta(\epsilon_F) \approx 8\ \text{eV}/N_{Au}$, so that $N_{Au} < 400$ atoms ($D < 2.5$ nm) is required so that the mean level spacing exceeds ambient temperature (0.025 eV). Accordingly, nearly all the extant knowledge has been obtained from cluster-beam experiments involving minute quantities of rigorously size (mass)-selected clusters in isolation, or from single-cluster measurements on supported clusters at cryogenic temperatures.

The rarity of the quantum-size effects among metal-based molecular and solid-state substances is primarily a result of the extreme difficulty in controlling cluster growth, structure, and surface passivation so as to isolate macroscopically obtained homogeneous clusters, without at some stage sacrificing the interesting properties. Apart from the striking example of the fullerenes (carbon clusters based essentially on the semimetal graphite structure), some success has been reported in obtaining massive metal clusters (Au, Pt, Pd)[7] via a ligand-based approach extended from small-cluster synthesis,[8] but these compounds involve halide or oxygen surface-chemical bonds that may "deaden" the surface metallic layer[9] and otherwise limit handling and measurements. A promising alternative employs the extended-surface chemistry based on amphiphilic adsorbates and which is known to lead to compact ordered monolayer structures

† Also at Instituto Physics, UNAM.

⊗ Abstract published in *Advance ACS Abstracts,* September 1, 1997.

S1089-5647(97)01438-7 CCC: $14.00

TABLE 1: Nanocrystal Core Dimensions (given by Mass,[a] Equivalent Diameter,[b] and Approximate Number of Atoms) and Its Characteristic Optical Absorption Features

Au core	SR[c]	sepn method	spectral characteristics[d] (eV) onset	features
8 *k* (1.1 nm, ~38 atoms)	SC_6	CC[e]		2.02,[f] 2.20, 2.39, 2.61
	SC_{12}			
	SC_{18}			
14 *k* (1.3 nm, ~75 atoms)	SC_4	FC[g]	1.6	1.77, 1.94, 2.21, 2.32, 2.60
	SC_6			
	SC_{12}			
	SC_{18}			
22 *k* (1.5 nm, ~101 atoms)	SC_6	FC	1.6	1.96, 2.27, 2.56
28 *k* (1.7 nm, ~146 atoms)	SC_6	FC	1.6	2.03, 2.21
	$SC\phi$[h]			
	SC_{12}			
	SC_{18}			
34−38 *k*	SC_6	FC	1.5	2.4[i] ± 0.2

[a] Onset/inflection point in the mass spectrum (see text for the units). [b] D_{eq} defined by $(\pi/6)D_{eq}^3 \bar{n}_{Au}^{fcc} = N_{Au}$. [c] Alkanethiol adsorbates. [d] d*A*/d*E* maxima. [e] Column chromatography. [f] Absorbance maximum. [g] Fractional crystallization. [h] Benzenethiol. [i] Obtained by subtracting a linear fit to the background absorption (cf. giant resonance of colloidal Au centered at 2.4 eV).

that do not substantially disrupt the geometric or electronic structure of the metal surface. The gold:thio (Au:SR) system is particularly ideal and well studied in this regard;[10] it combines this element's famously stable low-index surfaces and extreme electronegativity with a selective yet weakly binding adsorption group. In the ca. 4 years since this was proposed as a cluster-(nanocrystal)-based system, nc-Au:SR,[11] it has been obtained in various ways[12−14] and has been explored rapidly, particularly in the very large cluster range (~2^+ to 4 nm diameter).[15−20] The sub-2-nm range (<250 atoms) is, however, of greater interest for the quantum (QSE) properties, and also for molecular handling and characterization, including the potential for rigorous size separation and molecular-structure determination.

A major step in the exploration of the nc-Au:SR system was the 1995 report[15] that suitably prepared Au:SR cluster compounds could be isolated as a series of separable compounds, and several size-dependent structural, electronic, and spectroscopic properties have been reported on this series, which extends down toward 1.7 nm (~145 atoms) in ever-decreasing abundance. To overcome this limitation, some of us[21] briefly reported a refined preparation that produces a light series of three "critical size" Au:SR clusters, which inhibit further growth and thereby accumulate in very large abundances. These are denoted by their core masses, which lie in the ~14−30 *k* range, $k = 1000$ amu or 5.07 Au atoms, or equivalently by a diameter D_{eq} (1.3−1.7 nm range), or by the N_{Au} (~70−150). Mass-spectrometric evidence was also provided for an even smaller cluster obtained in much lower yield, with a core mass just below 8 *k* (38 Au atoms). (The various nomenclature for all the compounds mentioned below are summarized in Table 1.) Independently, Hostetler et al.[22] have arrived at a similar result using a different approach to controlling Au:SR cluster growth. Although preliminary evidence obtained on mixtures of this series indicated that the compounds have appealing properties (crystalline Au cores, tightly packed surfactant groups),[21,22] their exploration clearly requires separation according to size.

Here we report that these three main compounds, along with the smaller (8 *k*) one and a heavier mixture in the 34−38 *k* region, can indeed be isolated from each other to an extent that they exhibit a quantized energy-level structure in optical spectra. In a separate report we describe the observation of the discrete charging of these same molecular materials by electrochemical and tunneling spectroscopic methods.[23] These effects are new in that they are the properties of macroscopically obtained molecular materials, rather than results of single-molecule spectroscopy, and are not obscured by dispersity, thermal, decomposition, or relaxation effects.

2. Preparation, Separation, and Mass Analysis

The method of obtaining the series of smaller nc-Au:SR compounds in high (or exclusive) yield is essentially that described earlier,[21] based upon the procedures of ref 12, but with several important and comprehensible modifications. Here we describe the key aspects in an abbreviated form and give one detailed example.[24] The cluster growth process is essentially the solution-phase decomposition of a polymeric (or oligomeric) AuSR compound:

$$\left(\begin{matrix}\mathrm{R}\\ -\mathrm{AuS}-\end{matrix}\right)_p \rightarrow \mathrm{Au}_N(\mathrm{SR})_M + \mathrm{RSSR}, \quad 1.6 < N/M < 2.7 \quad (2)$$

which process is stimulated reductively under mild conditions (room temperature) by adding a reducing agent to an oil−water mixture. The crucial points to obtaining the smaller nanocrystals are the following: (i) the polymeric AuSR precursor in (2), which is used as prepared and has only modest solubility in toluene (depending on R), must be obtained *cleanly* (i.e., no residual Au^{III} chloride or excess thiol) by the precise stoichiometric reaction $3RSH + AuCl_4^- \rightarrow AuSR + RSSR +$ (acid and salt), i.e., with a 3:1 S:Au molar ratio; (ii) the reducing agent (aqueous $NaBH_4$) must be added all at once and in great molar excess to the vigorously stirred oil−water mixture; (iii) the successful addition and mixing will result in a very rapid change (on the order of 10 s) from colorless to opaque-brown-black; (iv) the effect of increasing (decreasing) temperature is to produce a relatively higher abundance of the larger (smaller) sizes; (v) with precise control of initial conditions, the terminal state (10^4−10^5 s) yields the desired smaller nanocrystals, but higher yields of the smallest cores are obtained by halting the reaction at an earlier stage (~10^3 s). These facts are consistent with principles of crystallite nucleation and multistage growth, as will be described separately; for further details on the relevant chemistry of Au, the reader is referred to ref 21 and to the earlier literature.

The resulting oil-soluble material can be precipitated from ethanol or acetone (depending on R) as a fine black crystalline powder, like typical nonpolar inorganic materials, and further washed with ethanol to remove byproducts or impurities, as confirmed by elemental analysis.[25] The materials prepared in this way show good thermal stability—a sample of 28 *k* Au:SC_6 was unaffected by hours in refluxing toluene ($T = 110$ °C)—and can be stored dry or in solution. Furthermore, the original SR monolayer can be *exchanged* with a distinct R*S group by dissolving the original material in a concentrated (or even neat) R*SH solution, and heating at ~80 °C for a few hours. Besides the functional group flexibility that this procedure affords, we have structural and decompositional evidence that this kind of treatment results in a more compact (saturated) and stable adsorbed monolayer.

The composition of the raw mixture of smaller nc-Au:SR compounds obtained in this way can be crudely assessed by low-resolution mass-spectrometric measurements, using the laser-desorption method described earlier,[15,26] as confirmed by other methods. An example of the compositional analysis of a raw mixture is given in the lowest frame (f) of Figure 1, and it is clear that this already shows the features identifying the main

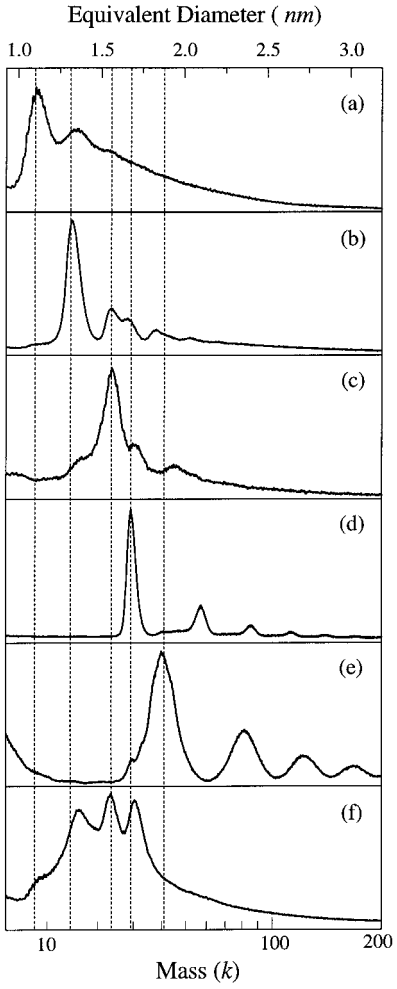

Figure 1. Low-resolution mass spectra, plotted as abundance vs (mass)$^{1/3}$, of size-separated clusters samples (b−e) and an unseparated raw mixture (a,f), obtained from growth of Au_N clusters from polymeric AuSR, where R is denoted by the *n*-alkyl chain length, C_n. The equivalent diameter of the cluster core (top axis) is calculated from the mass, assuming the density is that of bulk gold, and negelecting any contribution from bound SR groups retained, the dispersion in which is a prinicipal source of peak broadening. The primary peaks lie in the 5−44 *k* range, corresponding to $N = \sim 30-220$ atoms. The spectra are obtained by laser desorption time-of-flight mass spectrometry, with negative ion detection, performed on neat (matrix-free) films of the molecular solid; this results in a series of secondary or "coalescence"peaks at multiples and combinations of the primary masses. All mass spectra are calibrated against protein standards and are corrected for ejection velocity effects. The vertical dashed lines are provided to indicate the correspondence of the various principal peaks of each separated sample to the species detected in raw mixtures, as well as to the impurities remaining as molecularly mixed (not phase separated) substances. Estimates of the (percentage) abundances of the main species present in the samples are (a) 8 *k* (>75%), 14 *k* (<25%); (b) 8 *k* (∼5%), 14 *k* (80%), 22 *k* (15%); (c) 14 *k* (15%), 22 *k* (60%), 28 *k* (25%); (d) 28 *k* (95%), 38 *k* (<5%); (e) 28 *k* (∼10%); 34 *k* (∼30%), 38 *k* (∼60%); (f) example crude mixture includes 8 *k* (10%), 14 *k* (∼30%), 22 *k* (∼30%), 28 *k* (∼30%), >30 *k* (<10%). The R groups used in the preparation of the samples shown are (a) C_{12},(b) C_{18}, (c−e) C_6, (f) C_{12}.

constituents of the mixture. The tail toward higher mass results from the laser-induced aggregation of the cluster molecules, as can be seen clearly when they are analyzed as purified fractions. The use of ultrathin targets supported on a MALDI-type matrix results in complete supression of the higher-order (aggregation) peaks. The mixtures have been resolved, according to size (mass), by repeated fractional crystallization (FC), as accomplished by passive vapor transfer of a nonsolvent (acetone) to a solution (toluene) of the compounds. The entire process is monitored at each stage by laser-desorption mass spectrometry. The FC approach becomes less effective with decreasing core size and longer chain length. As a result, we have instead used liquid gravity column chromatography (CC, with toluene: THF as the mobile phase, neutral alumina packing) to obtain the highly purified 8 *k* Au:SC_6 compound. The results shown in Figure 1 indicate the level of separation that could be readily achieved by the former approach, for compounds with various n-alkyl chain lengths R = $(CH_2)_{n-1}CH_3 = C_n$. The resulting molecular materials are classified by core mass (associated with the steeper rising edge of the principal peak) as follows (see Table 1):

(i) The 14 *k* compound (Figure 1b), the smallest one obtained regularly as a macroscopically accumulated material, often near-exclusively under certain severely restricted conditions;

(ii) The 28 *k* compound (Figure 1d), easily obtained in high yield and often nearly the exclusive product of growth under slightly less restrictive conditions;

(iii) The 22 *k* compound (Figure 1c), never obtained in yields approaching those of (i or ii), and quite difficult to obtain in high purity from the others;

(iv) The 8 *k* compound (Figure 1a), which could only be obtained in high yield by an early termination (∼10^3 s) of the reaction; and

(v) A mixture of two or more compounds with onsets in the 34−38 *k* range (Figure 1e), included here primarily for comparison purposes.

In these mass spectra, the principal source of broadening of the main peak is the variable retention of the monolayer; very little Au atom loss is observed in high-resolution spectra (not shown).[26] Therefore, we have usually assigned the gold core mass from the midpoint or inflection of the rising edge of the main peak. However, in the case of the 8 *k* Au:SC_{12} compound, the rising edge is dominated by a resolved series of peaks with an onset near 7.5 *k* and a major spacing of 0.40 *k*; this pattern, which has been recorded several times (and at higher resolution) previously on low-yield light mixtures, is consistent with an assignment to a Au_{38} core and sequential RSSR (402 amu), although Au atom loss cannot be ruled out.

The identification of discrete compounds (as opposed to a closely overlapping mixture) is based upon three criteria: a single distinct rising edge (not multimodal) in each principal peak in individual mass spectra; the inability to accomplish even a partial further separation; and the repeatability of the same few features from widely varying preparations involving diverse thiols and other conditions. In particular, the same combination of inflections is seen in all samples (crude or separated), without any others in the 5−30 *k* range, suggesting that only four molecular species are accumulated in significant abundance across this range.

3. Further Characterization

Figures 2 and 3 show results from the further characterization—by high-resolution electron microscopy (HREM), scanning-tunneling microscopy (STM), and X-ray diffraction (XRD)—of selected samples of the molecular materials obtained and separated as described above. HREM and selected-area electron diffraction (ED) are among the most powerful tools for structural characterization of inorganic nanocrystals and large clusters adsorbed onto thin supports and have also been widely used for characterization of passivated nanocrystals with inorganic core dimensions exceeding ∼3 nm. The HREM investigation of smaller cluster molecules (<2.0 nm core dimension) that are quite inert (nonbinding) toward substrates presents difficulties not only from image contrast, momentum

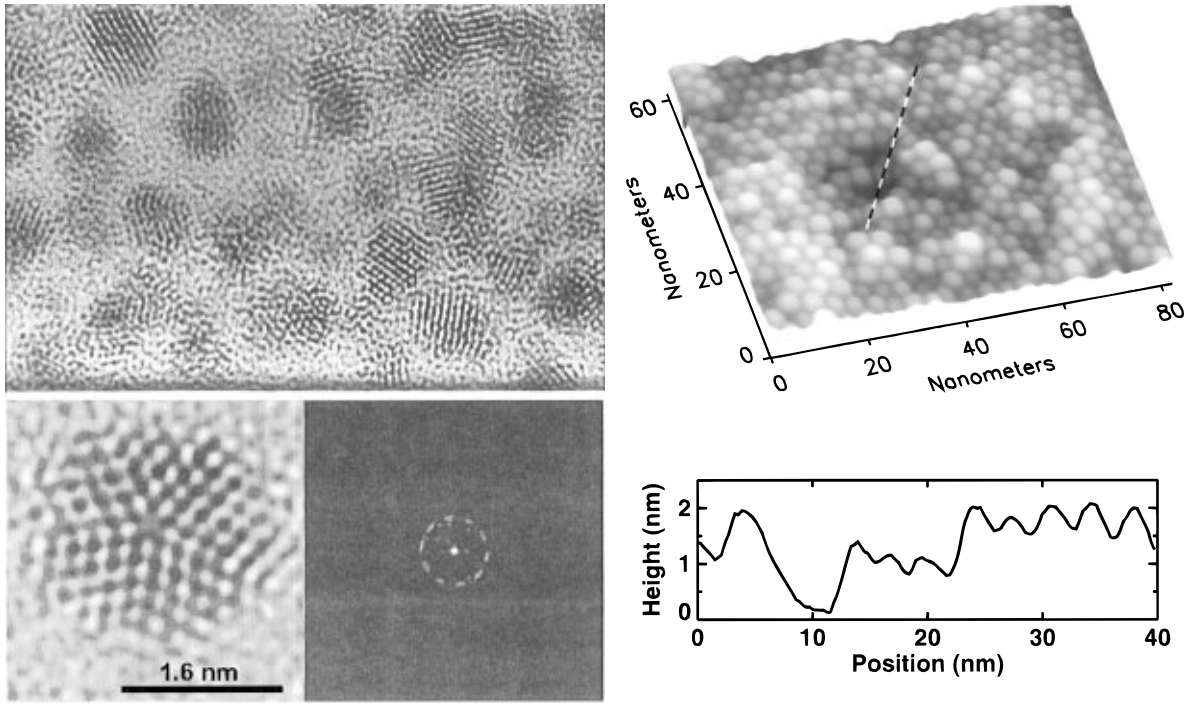

Figure 2. (a, left) High-resolution electron microscopy (HREM) images of smaller gold clusters Au:SC_{18} dispersed on amorphous carbon film, showing a field of crystalline gold cores in various orientations; the inset shows magnified image of a suitably oriented individual cluster core (ref 30). (b, right) Height-shaded STM image of a central portion of a large thin-film of 28 *k* Au:C_{12} clusters on graphite (HOPG) observed at $T = 300$ K. The tunnel current is 10 pA, and the substrate is biased at -1.0 V with respect to the tip. Well-ordered regions are apparent. The profile goes from lower-left to upper-right along the dashed line in the image. The zero elevation for the profile (suppressed) corresponds approximately to the HOPG surface. The ~3.5-nm periodicity evident from the profile corresponds well to that determined from XRD of thick films or powders of the same material.

transfer, and beam-damage considerations, but also from the intrinsic mobility of these giant molecules, as found by Luedtke and Landman in theoretical simulations of Au:SR molecules adsorbed onto graphite.[20] Nonetheless, a considerable effort has resulted in success at the level illustrated by Figure 2, which shows very small Au-cluster cores possessing considerable internal order, including many with projected dimensions close to those indicated by mass spectrometric, X-ray, and theoretical results.

XRD measurements on powder samples are shown in Figure 3, on samples corresponding to each of the mass spectra of Figure 1.[15,27,28] In the large-angle region (large s), the diffuse-peak patterns are reflective of the lattice structure of the Au cores, as the scattering effects of the low-mass S and C atoms are negligible by comparison. The maxima in these patterns can be associated with the Bragg reflections of bulk fcc-Au, and the feature widths are perfectly consistent the effective diameters indicated by mass spectrometry, assuming highly crystalline cores. The expected (Scherrer) FWHM, for Bragg reflections from ideal (strain-free) single-domain crystallites, is $\Delta s = 0.9\ D^{-1}$ or 0.8 to 0.4 nm^{-1} for crystallites in the $D =$ 1.1 to 1.9 nm range. Thus, these patterns can be taken to demonstrate, with high statistical significance, that the cores are crystalline (*not* amorphous or liquidlike). In a separate report, an extensive comparison has been made between the patterns (b−e) and a variety of proposed structural models, resulting in elimination of all except for truncated-decahedral (pentagonal-bipyramidal) family of quasicrystalline structures; the theoretical stability pattern for this family also provides a satisfying explanation for the occurrence of critical sizes at the masses found.[28] Pattern (a) and others obtained on 8 *k* rich samples suggest that its lattice structure is cubic-close-packed (fcc), which suggests a correspondence to the stability advantage of the 38-atom truncated octahedral structure in this size range.

In the small-angle region (small s), one finds in many cases a pattern of very strong, sharp peaks corresponding to the (super)lattice packing of the large molecules into ordered arrays. The observation of such a pattern depends crucially upon the quality of the separation of the mixture into purified molecular materials, and is enhanced by the use of shorter chains (SC_6 rather than SC_{12} or SC_{18}). The locations of the peaks give the lattice type, frequently bcc, and lattice constants; the intensities reflect mainly the size (and shape) of the giant scattering centers (gold cores) located on each (super)lattice site. In every case where a sufficiently large number (>6) of such peaks is observed to permit meaningful analysis, the intensities have been consistent with a single, globular (effectively spherical) Au core with a diameter close to that calculated from the observed masses (Figure 1) and the density of metallic Au. Furthermore, the distance between nanocrystal centers, as derived from the lattice constant and type, are consistent with a very dense packing of the monolayers around each core. Many further examples and analyses of such molecular crystal structures are given in the recent report of Shafigullin et al.[29]

Real-space STM imaging of such ordered structures is shown also in Figure 2, wherein a very thin film (3−4 molecular layers) of the 28 *k* Au:SC_{12} material gives rise to an observed "topography" with weak lateral ordering of globular entities and a typical center-to-center distance (3.5 nm) consistent with that determined from small-angle XRD patterns observed for the same material.

This structural characterization is in every way consistent with a picture of highly crystalline metallic Au cores encapsulated by a compact layer of weakly bound adsorbates. A complementary characterization of monolayer structures on these smaller nanocrystal Au molecules has been given recently by Hostetler et al.[22]

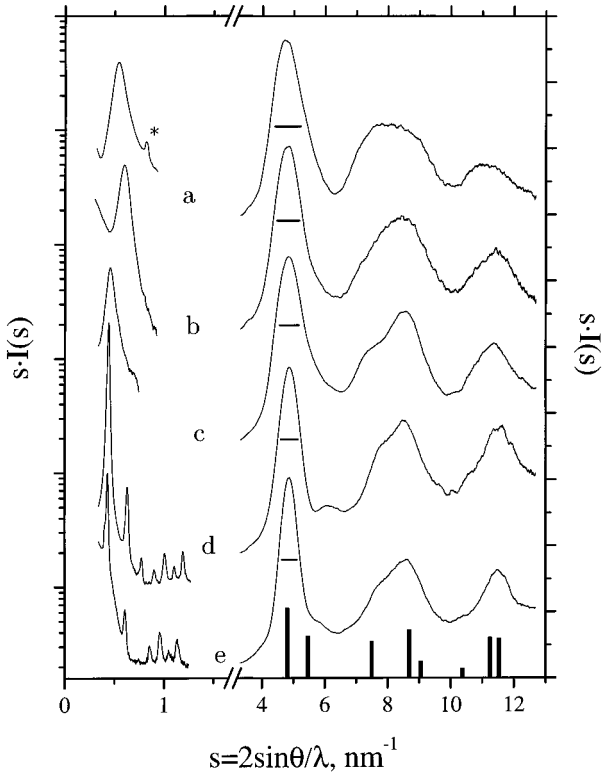

Figure 3. Powder XRD patterns plotted vs $s = 2 \sin \theta/\lambda$ (in nm^{-1}). In each panel, the patterns are given for the small *s* (left, on a logarithmic scale) and large *s* (right, on a linear scale) for the separated (a) 8 *k* Au:SC_6 (b) 14 *k* Au:SC_{18}, (c) 22 *k* Au:SC_6, and (d) 28 *k* Au:SC_6 samples, as well as for (e) the 34−40 *k* Au:SC_6 mixture (top to bottom, as in the first four frames of Figure 1). The bargraph (at bottom) indicates the reflections of bulk fcc-Au. Large-angle patterns are corrected for background, polarization, and geometry-dependent factors, and smoothed, and then offset from each other for ease of viewing. Horizontal bars indicate reflection widths (fwhm) expected on the basis of the crystallite diameters (see text). Small *s* patterns are shown as obtained, except that for pattern (d) a constant background of 0.02 × the peak maximum in *I*(*s*) has been subtracted.

4. Optical Spectra

Figure 4 shows a collection of optical absorption spectra in the electronic (1.1−4.0 eV) range, obtained on the new molecular materials described above, either in dilute toluene solution at room temperature[31] or as a neat film at $T = 8$ K. On a linear scale (upper frame), the spectra generally show an abrupt inflection upward at an energy (∼1.6 eV) corresponding to the interband transition edge, which marks the onset of transitions from the top of the $5d^{10}$ band to the lowest unoccupied levels of the broad 6sp conduction band, as diagrammed schematically in Figure 5. This characteristic value is observed not only for bulk (fcc) Au, but also for various Au_N clusters with as few as $N = 20$ atoms.[32,33] The threshold effect is brought out more clearly by plotting the spectra on a semilog scale (inset), so that the weaker (subthreshold) *intra*band absorption is evident. They generally show a *linear* increase in absorption intensity above threshold, which is already a frequently described characteristic of sub-2.5 nm Au crystallites prepared by various means.[34] The emergence of the plasmonlike feature in Au:SR nanocrystals with increasing size has already been described.[31]

In addition to these gross features, one finds for the smaller size-separated nanocrystal Au:SR molecules a steplike structure superimposed on the linear increase in absorption strength, with this structure becoming ever more pronounced with decreasing nanocrystal size. In the 14 *k* compound, it is readily evident even without close inspection. These spectral features are observed for all surfactant groups R (C_4, C_6, C_{12}, C_{18}, benzyl)

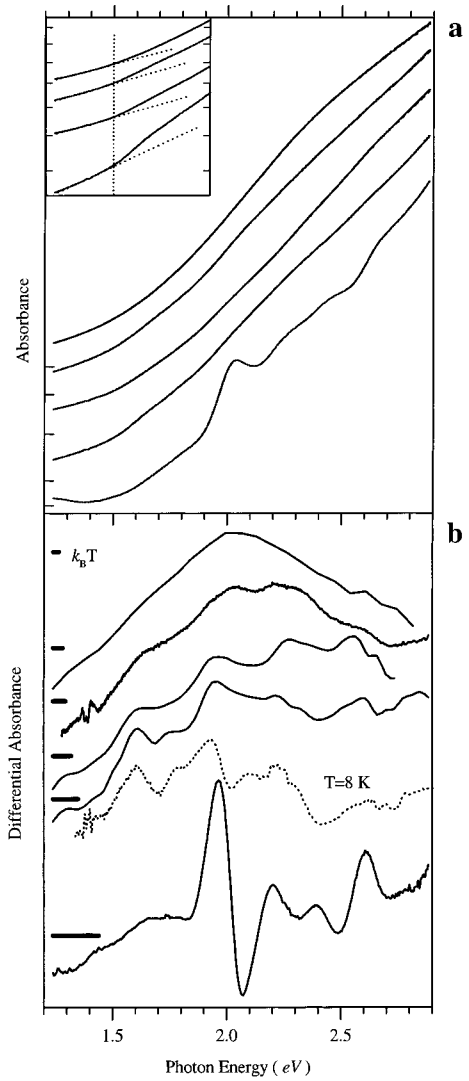

Figure 4. Optical absorption spectra, plotted on a linear (a), logarithmic (inset), and differential scale (b). The spectra have been normalized to unity absorbance at 4.0 eV, and then offset from each other for viewing (see true absorption zero markers at left of upper frame). In each part, the top four curves are (from top down) those for the 34−40 *k* mixture, the 28 *k*, the 22 *k*, and the 14 *k* samples (as in Figures 1 and 3), obtained in dilute toluene at room temperature. The lowest curve in both (a) and (b) is the spectrum of the chromatographically separated 8 *k* compound. The second-lowest curve (dotted line) in (b) is that for the 14 *k* Au:SC_{18} as a thin solid film, obtained at $T = 8$ K. The horizontal bars (−) in (b) indicate the thermal energy ($T = 300$ K) and the predicted mean-level spacings (δ) estimated from eq 1 for each core size.

with which the various masses have been obtained and purified. The 8-k compound shows an even more pronounced structure, in which not only steps but peaks emerge above the monotonically increasing suprathreshold absorption. All this structure can be brought out more clearly by plotting the differential absorption spectrum, as shown in Figure 4b. Also shown is the differential spectrum for the 14 *k* sample with SC_{18} groups prepared as a thin film and cooled to $T = 8$ K, which shows an enhancement in step structure.

In comparison to the preliminary picture presented earlier,[31] the evolution in spectral fine structure (Figure 4b) presented here has been greatly expanded by the inclusion of the 22 *k*, 34−40 *k*, and 8 *k* samples, by examining in at least one case the effect of temperature, and by comparing samples with various chain lengths (not shown). This allows a semiquantitative analysis of the spectra to be given:

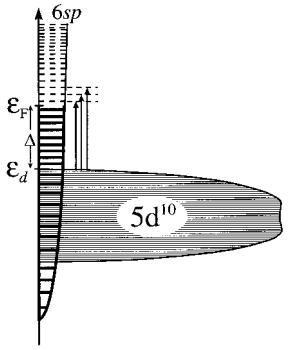

Figure 5. Schematic illustration of the band structure (orbital energy vs density of states) of fcc-Au, indicating the approximately correct bulk bandwidths and displacements, and density of states (solid curve). The discrete levels are indicated by solid (broken) lines below (above) the Fermi level ϵ_F, with a (mean) level spacing appropriate to a clusters of $N_{Au} \sim 50$ atoms. The vertical arrows designate optical transitions in the 1.7−2.5 eV range, originating at the top of the 5d band (ϵ_d) and terminating at each of the first few unoccupied levels. Adapted from the calculations and interpretation of ref 43.

First, the absorbance spectra have all been normalized to unity at high energies (4.0 eV), where the spectra no longer show any size-dependent variations. This is equivalent to normalizing to size (dividing by N), so that differential spectra can also be compared quantitatively to one another.[31]

Second, the steplike features in the spectra vary with core size not only in intensity but also in precise location, with the exception of the first feature (the interband onset), which is rather well aligned near 1.6 ± 0.1 eV. This means that mixtures of the samples are unlikely to resolve the steplike structure, which could therefore remain unnoticed.

Third, both the emergence of this structure and also the typical spacings among resolved features are consistent with the estimate for the mean energy-level spacing, eq 1, $\delta \sim 8$ eV/N, not considering degeneracies.[6] As the cluster size decreases from $N \sim 200$ to ~ 40, δ increases from 0.04 to 0.2 eV (see bars in Figure 4b) whereas the spacing must significantly exceed k_BT (∼0.025 eV at ambient temperature) in order that the spectra not involve *thermally excited* electronic states. The spectra of the larger clusters (upper two or three curves of Figure 4b) could therefore be interpreted as involving such states with a level structure too fine to be individually resolved. The fine structure of the 14 *k* material, both at room temperature and more clearly at cryogenic temperature, is consistent with resolving the expected number of energy levels (6−7 within 1.0 eV for a ∼75-atom cluster), and the lightest clusters (8 *k* Au:SC_6) might actually resolve all the energy levels.

Finally, the actual appearance of the spectral structure as *steps*, rather than *peaks*, and also their widths, should be explained in terms of the properties of the 5d band, which has an enormously greater (∼20×) density of states compared to the conduction band. Because these are not resolved on the 0.1 eV level in clusters of $N_{Au} > 20$ atoms,[32] the spectrum should be dominated by the discrete structure of the first unoccupied levels of the conduction band, as illustrated schematically in Figure 5. In this picture, each successively higher level represents a newly accessible channel from the top edge of the 5d band, assumed to be comparatively flat, thus leading to a cumulative or steplike increase in the total absorption. The differential spectra are then direct representations of the energy-level quantization (QSE) in the unoccupied portion of the conduction band. The width of these features as observed here may reflect the subpicosecond decay of the Auger-like excitation, as has already been inferred for smaller gold nanocrystals excited at higher photon energies,[35] in addition to extrinsic (residual inhomogeneities in the material, or thermal) effects. Of course, this discrete level structure could alternatively be obtained by other methods, including high-resolution inverse-photoemission spectroscopy, tunneling spectroscopy, or direct optical spectroscopy in the intraband (mid-IR) region.

5. Discussion and Conclusions

The high-yield isolation of individual members from a series of massive gold-cluster Au:SR molecules, with crystalline cores, ranging in size from ∼1.1 nm (∼40 atoms) to ∼1.9 nm (∼200 atoms), has been accomplished by decomposition of a polymeric precursor followed by fractional crystallization as monitored by high-mass spectrometry and characterization by methods including X-ray diffraction (small and large angle), high-resolution electron microscopy, and scanning tunneling microscopy. Further efforts toward quantitative separations, precise composition determinations, and structural characterizations are in progress. These thermally, photochemically, and environmentally stable molecular materials can be investigated as molecular crystals, on solid substrates, in the gas phase (by cluster beam methods),[26,32] or in solution as reported herein.

The visible spectrum, or color, of gold in all its condensed forms (bulk, thin films, colloidal particles, gas-phase clusters) is dominantly derived from interband transitions originating in the filled and submerged 5d^{10} band and terminating in unoccupied states of the 6(sp)^1 conduction band.[34,36] Accordingly, we have found that optical absorption spectra of dilute solutions containing these molecules show a size-dependent steplike structure originating near the interband edge ($\Delta = 1.7$ eV) of bulk or cluster Au.[32,33] This structure is evident in the smallest clusters even at room temperature, is enhanced at low temperature, and can be interpreted as the discrete energy levels corresponding to the first unoccupied orbitals of the delocalized conduction electrons, i.e., as a direct manifestation of the quantum size effects in a macroscopic sample of metal clusters. Experiments on mass-selected cluster beams include many examples of structured optical spectra, usually on smaller clusters, involving *intraband transitions* at a correspondingly higher level of excitation energy.[37] Tunneling measurements on *single* metal particles have also revealed energy level fine structure, but only at cryogenic temperatures.[38] Our results are unusual in that they involve macroscopically obtained cluster-molecule materials which show structured spectra even at normal temperatures.

It is important here to distinguish this interpretation of nonbulk electronic structure in metal clusters from one involving a change in the *nature of the bonding* from metallic, i.e., nondirectional and based on highly delocalized conduction electrons, to nonmetallic (directional and/or based on localized electrons). The latter metal−nonmetal transition occurs, for example, as a result of a strong rehybridization in the larger clusters (∼13−40 atoms) of certain group II and III metals (Hg, Al, etc.),[39] and is also envisaged to occur in a more trivial manner if the exposed (surface) atoms of the cluster are involved in surface chemical bonds with strongly electronegative atoms (halides, oxides) resulting in a "dead" surface layer.[9] We are aware of no evidence that Au:SR clusters and nanocrystals undergo any such metal−nonmetal transition; on the contrary, Au and S are equally electronegative S, so the surface bond (which is not well understood for the Au:SR class of systems[10]) is unlikely to be a "thiolate" ($Au^+-{}^-SR$); XPS results show no evidence of any "oxidized" Au atoms; and the electronic level structure revealed here spectroscopically is entirely consistent with a conduction electron number and density close to that of bulk fcc-Au, despite the absence of a broad "plasmon"-

like band centered at 2.4 eV that is often taken loosely to be the signature of metallic gold spheres. We expect that for the smallest Au:SR cluster molecules (~38 Au atoms) these issues can be resolved decisively by a combination of first-principles theoretical and continued experimental investigations founded on precise structural information, as already demonstrated for the large metalcarbonyls, e.g. the truncated-octahedral compound $Pt_{38}(CO)_{44}$ with a cubic close-packed core.[40]

Concerning the detailed interpretation of the energy-level pattern, it is interesting that the quantization of conduction-band energy levels in metal *and* semiconductor nanocrystals has led to *both* classes of materials being labeled crudely as "quantum dots" or "artificial atoms", although the level of complexity is strikingly different. For semiconductor nanocrystals,[41] the energy-level pattern observed spectroscopically, employing valence-to-conduction (interband) transitions, reveals only the lowest few levels of the (normally empty) conduction band; these are rather insensitive to the shape and lattice structure of the nanocrystal, and in any case they are unimportant for the behavior of the nanocrystal at ordinary temperatures. In metal nanocrystals the level pattern near the highest occupied level is critically sensitive to the shape of the crystallite and is essential to describing its properties (thermal, chemical, electrochemical) even in the absence of optically induced electronic excitations or doping.[6] Thus, a quantitative interpretation of spectral structure, such as that observed here, requires a detailed comparison with quantum calculations of level structure for various structural models, but in turn can yield much valuable information underlying a manifold of important properties of the nanocrystals individually and in arrays or molecular crystals. Ongoing low-temperature measurements (optical and tunneling spectroscopy[42]) will give a clearer picture of the conduction band, enabling a detailed comparison with various structures and level fillings.

Acknowledgment. This research has been supported by the Office of Naval Research, the Packard Foundation, and the Georgia Tech Research Foundation. For their contributions to various aspects of this work, the authors are indebted to Dr. Marcos M. Alvarez (preliminary investigations); Dr. S. Logunov and Prof. M. A. El-Sayed (optical spectroscopy); Dr. M. Hostetler (unpublished manuscripts); Dr. A. Chemseddine (preparation kinetics and separations); Profs. A. Wilkinson and P. Stephens (X-ray diffractions); and Prof. U. Landman and W. A. deHeer (critical advice on electronic structure and excitations).

References and Notes

(1) See articles in: *Clusters of Atoms and Molecules*, Haberland, H., Ed.; Springer Series in Chemical Physics 52 and 57; Springer: Berlin, 1994.
(2) Landman, U.; Luedtke, W. D.; Salisbury, B. E.; Whetten, R. L. *Phys. Rev. Lett.* **1996**, *77*, 1362, and references therein.
(3) Martin, T. P. *Phys. Rep.* **1996**, *273*, 199−241.
(4) Parks, E. K.; Winter, B. J.; Klots, T. D.; Riley, S. J. *J. Chem. Phys.* **1991**, *94*, 1882.
(5) Näher, U.; Göhlich, H.; Lange, T.; Martin, T. P. *Phys. Rev. Lett.* **1992**, *68*, 3416.
(6) (a) deHeer, W. A. *Rev. Mod. Phys.* **1993**, *65*, 611−676. (b) Kubo, R.; Kawabata, A.; Kobayashi, S. *Annu. Rev. Mater. Sci.* **1984**, *14*, 49.
(7) Schmid, G.; Morun, B.; Malm, J.-O. *Angew. Chem., Int. Ed. Engl.* **1989**, *28*, 778−780.
(8) Teo, B. K.; Shi, X.; Zhang, H. *J. Am. Chem. Soc.* **1992**, *113*, 2743.
(9) Mulder, F. M.; Stegink, T. A.; Thiel, R. C.; de Jongh, L. J. *Nature* **1995**, *367*, 716.
(10) Dubois, L. H.; Nuzzo, R. G. *Annu. Rev. Phys. Chem.* **1992**, *43*, 437−463. Fenter, P.; Eberhardt, A.; Eisenberger, P. *Science* **1994**, *266*, 1216.
(11) Whetten, R. L. Presented at the NEC Conference on New Material Phases, Karuizawa, Japan, October 1992; *Mater. Sci. Eng.* **1993**, *B19*, 8−13.
(12) Brust, M.; Walker, M.; Bethell, D.; Schiffrin, D. J.; Whyman, R. *J. Chem. Soc., Chem. Commun.* **1994**, 801.
(13) Andres, R. P.; Bein, T.; Dorogi, M.; Feng, S.; Henderson, J. I.; Kubiak, C. P.; Mahoney, W.; Osifchin, R. G.; Reifenberger, R. *Science* **1996**, *272*, 1323−5.
(14) Alvarez, M. M. Dissertation, UCLA, 1995. Harfenist, S. A.; Wang, Z. L.; Alvarez, M. M.; Vezmar, I.; Whetten, R. L. *J. Phys. Chem.* **1996**, *100*, 13904.
(15) Whetten, R. L.; Khoury, J. T.; Alvarez, M. M.; Murthy, S.; Stephens, P. W.; Vezmar, I.; Wang, Z. L.; Cleveland, C. L.; Luedtke, W. D.; Landman, U. In *Chemical physics of fullerenes*; Andreoni, W., Ed.; Kluwer: Dordrecht, 1996; pp 475−490; *Adv. Mater.* **1996**, *8*, 428−433.
(16) Terrill, R. H.; Postlethwaite, T. A.; Chen, C.-H.; Poon, C.-D.; Terzis, A.; Chen, A.; Hutchison, J. E.; Clark, M. R.; Wignall, G.; Londono, J. D.; Superfine, R.; Falvo, M.; Johnson, C. S.; Samulski, E. T.; Murray, R. W. *J. Am. Chem. Soc.* **1995**, *117*, 12537.
(17) Badia, A.; Singh, S.; Demers, L.; Cuccia, L.; Brown, G. R.; Lennox, R. B. *Chem.-Eur. J.* **1996**, *2*, 205.
(18) Brust, M.; Bethell, D.; Schiffrin, D. J.; Kiely, C. J. *Adv. Mater.* **1995**, *7*, 795.
(19) Leff, D. V.; Ohara, P. C.; Heath, J. R.; Gelbart, W. M. *J. Phys. Chem.* **1995**, *99*, 7036.
(20) Luedtke, W. D.; Landman, U. *J. Phys. Chem.* **1996**, *100*, 13323.
(21) Alvarez, M. M.; Khoury, J. T.; Schaaff, T. G.; Shafigullin, M. N.; Vezmar, I.; Whetten, R. L. *Chem. Phys. Lett.* **1997**, *266*, 91−8. Fitch, H. M. U.S. Patent Nos. (2,994,614; 2,984,575) 1961.
(22) Hostetler, M., et al. *Langmuir*, in press.
(23) Ingram, R., et al. *J. Am. Chem. Soc.*, in press.
(24) As a concrete example, 537 mg of tetraoctylammonium bromide in 65 mL of toluene is added with stirring to 79 mg of $HAuCl_4$ in 10 mL of H_2O, until the organic layer is deep red and the aqueous layer (formerly yellow) is colorless, after which *n*-dodecanethiol (154 mL) is added, with further stirring, corresponding to a 2.95:1 molar ratio (S:Au), resulting in a complete loss of the red color and a slightly cloudy organic layer. This mixture is stirred for ~20 min, after which is added 230 mg of $NaBH_4$, dissolved in 4 mL of H_2O, with further vigorous stirring, resulting in a rapid change to a opaque brown solution. The composition of the massive clusters generated is monitored by extracting small samples on a time scale of a few minutes to several days; these are washed with ethanol, redissolved in toluene, and analyzed mass spectrometrically as described in the text. After 15 min the analysis of this particular preparation shows predominantly the 14 *k* compound, along with indications of much lighter unresolved material. After several hours the 22 *k* is predominant, and after 1 day the 28 *k* is also strongly observed.
(25) Elemental analysis (Galbraith Laboratories) of a 28 *k* Au: SC_6 sample showed mass fractions for C (0.1126), H (0.0211), S (0.0515), and Au (0.8184), with impurities from other starting materials totaling to <0.02. Molar ratios found for S:C (5.84:1) and H:C (2.23:1) agree well with the 6:1 and 2.2:1 ratios calculated for the thiol(ate), whereas the 2.57:1 ratio for Au:S would indicate that a cluster of ~145 atoms has a coverage of ~56 thiol(ate) groups.
(26) Vezmar, I.; Alvarez, M. M.; Khoury, J. T.; Salisbury, B. E.; Schaaff, T. G.; Whetten, R. L. *Z. Phys.* **1997**, *D40*, 147.
(27) Cleveland, C. L.; Landman, U.; Shafigullin, M.; Stephens, P. W.; Whetten, R. L. *Z. Phys.* **1997**, *D40*, 503.
(28) Cleveland, C. L.; Landman, U.; Schaaff, T. G.; Shafigullin, M.; Stephens, P. W.; Whetten, R. L. *Phys. Rev. Lett.*, in press. Doyes, J. P. K.; Wales, D. J. *Chem. Phys. Lett.* **1995**, *247*, 339.
(29) Shafigullin, M., et al., submitted for publication.
(30) Ascensio, J., et al. *Surf. Sci.*, in press.
(31) Alvarez, M. M.; Khoury, J. T.; Schaaff, T. G.; Shafigullin, M. N.; Vezmar, I.; Whetten, R. L. *J. Phys. Chem.* **1997**, *101*, 3706.
(32) Taylor, K. J.; Pettiette-Hall, C. L.; Cheshnovsky, O.; Smalley, R. E. *J. Chem. Phys.* **1992**, *96*, 3319.
(33) Häberlen, O. D.; Chung, S.-C.; Rösch, N. *Ber. Bunsen-Ges. Phys. Chem.* **1994**, *98*, 882−5. Häberlen, O. D.; Chung, S.-C.; Stener, M.; Rösch, N. R. *J. Chem. Phys.* **1997**, *106*, 5189.
(34) Kreibig, U.; Vollmer, M. Optical Properties of Metal Clusters; Springer: Berlin, 1995.
(35) Logunov, S.; Ahmadi, T. S.; El-Sayed, M. A.; Khoury, J. T.; Whetten, R. L. *J. Phys. Chem.* **1997**, *101*, 3713.
(36) Ashcroft, N. W.; Mermin, N. D. Solid State Physics; Saunders: New York, 1976; Chapter 15.
(37) Ellert, C.; Schmidt, M.; Schmitt, C.; Reiners, T.; Haberland, H. *Phys. Rev. Lett.* **1995**, *75*, 1731.
(38) Ralph, D. C.; Black, C. T.; Tinkham, M. *Phys. Rev. Lett.* **1995**, *74*, 3241.
(39) Schriver, K. E.; Persson, J. L.; Honea, E. C.; Whetten, R. L. *Phys. Rev. Lett.* **1990**, *64*, 2540.
(40) Roth, J. D.; Lewis, G. J.; Safford, L. K.; Jiang, X.; Dahl, L. F.; Weaver, M. J. *J. Am. Chem. Soc.* **1992**, *114*, 6159. See also: Parks, E. K.; Nieman, G. C.; Kerns, K. P.; Riley, S. J. *J. Chem. Phys.* **1997**, *107*, 1861.
(41) For review, see: Alivisatos, A. P. *J. Phys. Chem.* **1996**, *100*, 13226.
(42) First, P. N., et al., manuscript in preparation.
(43) Christensen, N. E.; Seraphin, B. O. *Phys. Rev.* **1971**, *B4*, 3321.